

ISSN 2063-5346



HEAT TRANSFER MECHANISM OF WILLIAMSON HYBRID NANOFLUID FLOW ACROSS A NONLINEARLY EXTENDING SURFACE WITH RADIATION EFFECTS

Sunita J¹, Suresh Biradar^{1*} and Samrat SP²

Article History: Received: 10.05.2023

Revised: 29.05.2023

Accepted: 09.06.2023

Abstract

In this study, we examined the radiative MHD Williamson hybrid nanofluid flow over an uneven stretching surface with the nonlinear heat source. The hybrid nanofluid is composed of MoS₂ and Ag suspended in ethylene glycol. The similarity variables are used to transmit PDE's to ODE's and resolved by adopting R-K method with the shooting technique. Further, the stimulus of physical parameters on dimensionless quantities like momentum, thermal, wall friction and Nusselt number are discussed thru plots and tables. Results reveal that decreasing velocity and rising temperature are found by considering larger magnetic properties. The volume fraction tends to develop conductance of the hybrid nanofluid. The hybrid nanofluid shows a higher flow and heat transmission rate as compared to the mono nanofluid.

Keywords: Hybrid nanofluid, MHD, radiation, nonlinearly stretching surface, uneven heat rise\fall.

¹Department of Mathematics, Sharanbasva University, Kalaburagi, Karnataka, India 585103.

²Department of Mathematics, Shri Prabhu Arts, Science & JM Bohra Commerce College Shorapur, Karnataka, India 585224

DOI:10.48047/ecb/2023.12.9.44

1. Introduction

The significance of heat flow has excellent applications in production and manufacturing science. The fluids like water, ethylene glycol, kerosene, engine oil, etc are used to control the consequences of heat cooling and rising factors. It's a traditional culture to utilize these and there are no choices, but these outcomes have less efficiency in heat command. We can't ignore any of these due to the huge availability in nature. In 1995, Choi [1] invented a revolutionary nanofluid which overcomes all such drawbacks of normal fluids. Nanofluid is the combination of normal fluid and metallic/non-metallic particles which enhances 40% of heat transmission. Later, Fersadou et al. [2] considered the entropy production and MHD convection of nanofluid in vertical porous channels. Also, Patil et al. [3] discussed the surface unevenness property of mixed convective nanofluid flow over an elongating surface with suction and injection impacts. Sudarsana et al. [4] analyzed the magnetized mass and thermal flow of nanofluid on a vertical plate immersed in porosity under various physical aspects. Samrat et al. [5] studied the radiation property of the wavering flow of Casson nanofluid over an elongating surface.

A usual nanofluid does not perform well in today's computation and requirements due to its limited properties. The researchers have invented another fluid named hybrid nanofluid. It accomplishes the weakness of the nanofluid. It is comprised of mixtures of two different nanoparticles into the base liquids. Waqas et al. [6] studied the heat transport of hybrid nanofluids flow over a vertical stretching cylinder by implementing the Tiwari and Das model. Rashid et al. [7] proposed that the different shape of the nanoparticles and hybridization of nanofluid amplifies the performance of heat transference. Ullah et al [8] discussed numerically the flow of hybrid nanofluids over an extended

surface. Jamaludin et al. [9] analyzed the stagnation point flow of a hybrid nanofluid (Cu-Al₂O₃-H₂O) over a shrinking/stretching surface with MHD and heat sink/source. Sulochana et al. [10] analyzed the boundary layer flow of a nanofluid over a constantly stirring slender needle.

Heat transmitting properties on a hybrid-nanofluid over an elongating sheet have loads of uses in industrial science due to their individuality. Thermal and momentum profiles are controlled by stretching properties. Heat transmits more when the stretching parameter is increased. Tlili et al. [11] studied numerically that MHD dissipative flow on an extended region in the occurrence of Soret/Dufour effects. They found that these effects control the diffusion and thermal fields. Waini et al. [12] studied flow and heat variations of hybrid nanofluids thru permeable stretching surfaces. They found that hybrid nanofluids have higher heat variations compared to the mono nanofluids. The boundary layer flow and thermal properties of nanofluids over an uneven elongating sheet were studied numerically by Mabood et al. [13]. It is found that Brownian motion enhances when the thickness of the boundary layer increases. Hayat et al. [14] discussed the 3D flow of mixed convective Williamson nanofluid over a stretched region with a chemical reaction. Tlili et al. [15] explored the MHD effects on hybrid nanofluid i.e. (CuO+MgO+Methanol), over the uneven surface.

Further, MHD has a wide variety of applications in metallurgy, mining of geothermal energy, metal casting, medicine, polymer industry, melting and fusion reactor etc. Alghmdi et al. [16] reported that hybrid nanofluid flow with magnetic effects is used in the medication of blood arteries. Shoaib et al [17] investigate the MHD effects on hybrid nanofluids on a rotating stretching surface with radiation. Later, Aly and Pop [18]

employed MHD effects near a stagnation region over an extended surface with viscous dissipation and compared the results of hybrid nanofluid and single nanofluid. Moreover, Ashwinkumar et al [19] studied convective hybrid nanofluid with magnetic effects in two, unlike geometries. Further, Ghadikolaei et al [20] discussed the shape and size of nanoparticles importance in stagnation point flow with magnetic properties. Sandeep et al [21] studied flow and heat properties in MHD (magnetohydrodynamics) dusty hybrid ferrofluids with radiation effects.

In view of the above studies, we employed the radiative MHD Williamson hybrid nanofluid flow over an irregular extending surface with a nonlinear heat source. The similarity variables are used to transmit PDE's to ODE's and resolved by adopting R-K method with the shooting technique. Further, the effects of physical

parameters on dimensionless quantities like momentum, thermal, friction factor and Nusselt number are discussed thru plots and tables. Results reveal that the heat transfer rate of hybrid nanofluids shows a better response as related to the single nanofluid.

2. Mathematical modelling

We presumed steady, hydrodynamic stream of Williamson hybrid nanofluid flow above a nonlinear extending surface with radiative heating and uneven heat source effect. The varying magnetic force and elongating are given by $U_w = ax^n$ and $B(x) = B_0x^{2n-1}$ respectively. The surface temperature $T_w = T_\infty + bx^{2n-1}$, T_∞ is the free stream temperature. Influence of radiative heating, irregular heat source is computed in the energy equation.

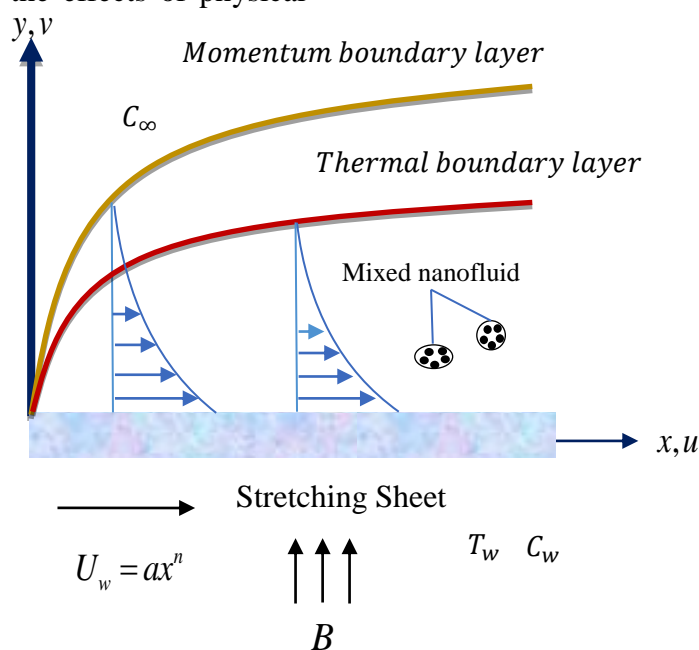


Fig.1 Flow geometry of the problem

Under the above presumptions the stream and energy transport featured equations are stated as Jafar, et al [22]

$$\frac{\partial u}{\partial x} + \frac{\partial v}{\partial y} = 0, \tag{1}$$

$$\rho_{hmf} \left(u \frac{\partial u}{\partial x} + v \frac{\partial u}{\partial y} \right) = \mu_{hmf} \left(1 + \sqrt{2}\Gamma \frac{\partial u}{\partial y} \right) \frac{\partial^2 u}{\partial y^2} - \sigma_{hmf} B_0^2(x) u, \quad (2)$$

$$(\rho c_p)_{hmf} \left(u \frac{\partial T}{\partial x} + v \frac{\partial T}{\partial y} \right) = k_{hmf} \frac{\partial^2 T}{\partial y^2} - \frac{\partial q_r}{\partial y} + q''' , \quad (3)$$

respective edge restrictions,

$$\left. \begin{aligned} u = U_w(x) = ax^n, v = 0, T = T_w = T_\infty + bx^{2n-1} \text{ at } y = 0 \\ u \rightarrow 0, T = T_\infty \text{ as } y \rightarrow \infty \end{aligned} \right\}, \quad (4)$$

where the sheet is mounted along x direction along the sheet, y is normal to the sheet, with velocity components as u and v respectively. While q''' is the irregular heat rise/fall parameter and is expressed as,

$$q''' = \frac{k_{hmf} U_w}{\nu_f} \{ A(T_w - T_\infty) F' + B(T - T_\infty) \}, \quad (5)$$

where A, B is the space and time dependant heat source sink parameters.

The non-dimensional similarity variables are stated as below,

$$\left. \begin{aligned} u = ax^n F'(\eta), v = -\sqrt{\frac{av(n+1)}{2}} x^{0.5(n-1)} \left(F + \frac{n-1}{n+1} \eta F' \right), \\ \eta = y \sqrt{\frac{a(n+1)}{2\nu}} x^{0.5(n-1)}, \Theta(\eta) = \frac{T - T_\infty}{T_w - T_\infty}, \end{aligned} \right\}, \quad (6)$$

where η is the similarity factor.

The thermophysical features of mixed nanofluid are specified as Ashwinkumar et al. (2022),

$$\left. \begin{aligned} \frac{\mu_{hmf}}{\mu_f} &= \frac{1}{(1-\phi_1)^{5/2} (1-\phi_2)^{5/2}}, \quad \frac{\rho_{hmf}}{\rho_f} = \frac{\rho_{s_2}}{\rho_f} \phi_2 + (1-\phi_1)(1-\phi_2) + \frac{\rho_{s_1}}{\rho_f} \phi_1 (1-\phi_2), \\ \frac{k_{hmf}}{k_{nf}} &= \frac{k_{s_2} + 2k_{bf} - 2(k_f - k_{s_2})\phi_2}{(k_f - k_{s_2})\phi_2 + 2k_f + k_{s_2}}, \quad \frac{k_{nf}}{k_f} = \frac{k_{s_1} + 2k_f - 2(k_f - k_{s_1})\phi_1}{2k_f + (k_f - k_{s_1})\phi_1 + k_{s_1}}, \\ \frac{(\rho c_p)_{hmf}}{(\rho c_p)_f} &= \frac{(\rho c_p)_{s_2}}{(\rho c_p)_f} \phi_2 + (1-\phi_1)(1-\phi_2) + \frac{(\rho c_p)_{s_1}}{(\rho c_p)_f} \phi_1 (1-\phi_2), \\ \frac{\sigma_{hmf}}{\sigma_f} &= \left[1 + \frac{3\sigma_{s_1}\phi_{s_1} + \phi_{s_2}\sigma_{s_2} - \phi\sigma_f}{\sigma_{s_1}(1-\phi_{s_1}) + \sigma_{s_2}(1-\phi_{s_2}) + (2+\phi)\sigma_f} \right], \end{aligned} \right\}, \quad (7)$$

where the suffixes $_{hmf, nf, f}$ describes the hybrid nanofluid, mono nanofluid and base fluid respectively.

By utilizing Eqn. (5) - (7) in Eqn. (2) and (3), we get,

$$(1 + WeF''') F''' + \frac{\rho_{hmf} \mu_f}{\rho_f \mu_{hmf}} \left(FF'' - \left(\frac{2n}{n+1} \right) F'^2 \right) - \frac{\sigma_{hmf}}{\sigma_f} MF' = 0, \quad (8)$$

$$\left(\frac{k_{hmf}}{k_f} + R \right) \Theta'' + \text{Pr} \frac{(\rho c_p)_{hmf}}{(\rho c_p)_f} \left\{ F \Theta' - \left(\frac{2(2n-1)}{n+1} \right) F' \Theta \right\} + AF' + B\Theta = 0, \quad (9)$$

the transmuted edge restrictions are,

$$\left. \begin{aligned} F(\eta) = 0, \quad F'(\eta) = 1, \quad \Theta(\eta) = 1 \quad \text{at } \eta = 0 \\ F'(\eta) = 0, \quad \Theta(\eta) = 0, \quad \text{as } \eta \rightarrow \infty, \end{aligned} \right\}, \quad (10)$$

here $\phi, n, M, We, \text{Pr}$, are the nanoparticle volume fraction, nonlinear stretching, magnetic force, Weissenberg number, Prandtl number respectively are quantified as below,

$$M = \frac{2\sigma_f B_0^2}{a(n+1)\rho_f}, \quad We = \Gamma a^{1.5} x^{\frac{(3n-1)}{2}} \left(\frac{n+1}{\nu_f} \right)^{0.5}, \quad \text{Pr} = \frac{(\mu c_p)_f}{k_f}, \quad (11)$$

The physical factors of practical concern are C_{fx} and Nu_x are outlined as,

$$C_{fx} = \frac{\tau_w}{\rho_f \mu_w^2} \quad \text{and} \quad Nu_x = \frac{xq_w}{k_f (T_w - T_\infty)}, \quad (12)$$

where τ_w and q_w are given by,

$$\left. \begin{aligned} \tau_w = \mu_{hmf} \left(\frac{\partial u}{\partial y} + \frac{\Gamma}{\sqrt{2}} \left(\frac{\partial u}{\partial y} \right)^2 \right)_{y=0}, \quad q_w = -k_{hmf} \left(\frac{\partial T}{\partial y} \right)_{y=0} \end{aligned} \right\}, \quad (13)$$

The simplified form of C_{fx} and Nu_x are listed as,

$$\left. \begin{aligned} \text{Re}_x^{0.5} C_{fx} &= \frac{\mu_{hmf}}{\mu_f} \left(\frac{n+1}{2} \right)^{0.5} \left(F''(0) + \frac{We}{2} (F''(0))^2 \right), \\ \text{Re}_x^{-0.5} Nu_x &= - \left(\frac{k_{hmf}}{k_f} + R \right) \left(\frac{n+1}{2} \right)^{0.5} \Theta'(0) \end{aligned} \right\}, \quad (14)$$

where $\text{Re}_x = xu_x(x)/\nu_f$ is the Reynolds number.

3. Results and discussion

In this section, the impact of non-dimensional parameters like power-law index (n), thermal radiation (R), magnetic field (M), non-uniform heat source (A, B), volume fraction (ϕ_1, ϕ_2) on stream and temperature of the nano and hybrid nanofluids are analyzed via plots and also the impression of these parameters on skin friction factor and thermal transport rate are depicted in the tabular form. The numerical computations are discussed by

keeping $We = 0.5, R = 0.5, A = 0.5, B = 0.4, n = 3, M = 2, \phi_1 = \phi_2 = 0.05$ throughout the complete study. The main objective of this research article is to deliberate the comparative outcomes of nanofluids with the hybrid nanofluids.

Figs. 2-3 depict the impression of n on stream and temperature gradients for mono nonfluid and hybrid nanofluid. It is documented that both flow and energy gradients are opposite in nature. The velocity is declined whereas temperature is

amplified for constructive values of n . Figs. 4-5 represents the power of M on $F'(\eta)$ and $\theta(\eta)$. We observe that fluid velocity is deteriorated and energy is improved for positive values of M . Physically increase in M creates a resistive type of force termed as Lorentz force which slow down the motion of the fluid.

The responses of We on $F'(\eta)$ and $\theta(\eta)$ are represented in the figs. 6-7. For higher magnitudes of We , fluid stream is lessened and thermal gradient is boosted. Hike in We increases the relaxation time of the fluid particles so that viscosity is enhanced reducing the fluid flow. Figs. 8-9 portray the impression of non-uniform heat source parameter on thermal gradient. The cumulative values of A and B acts as heat generators, which increases the temperature of the fluid. Further, the rise in the energy is same for both nanofluid and hybrid nanofluid. The significance of R on $\theta(\eta)$ is illustrated from the fig.10. The supplementary value of radiation parameter augments the heat energy of the fluid which results in advancing the fluid temperature.

The thermo physical attributes of MoS_2 and Ag nanoparticles along with carrier fluid engine oil are listed in the table 1. Moreover, Table 2 is drawn to study the variation in the skin friction factor for fluctuating values of physical parameters. It is witnessed from the table that C_{fx} is the accelerating function of Weissenberg number whereas deaccelerating function of magnetic field and power law index parameters. Further, no change is recorded for magnifying values of thermal radiation for both nanofluid and hybrid nanofluids.

Table 3 denotes the variation in the thermal transfer rate for diverse values of the physical parameters. From the table we observe that Nusselt number is the diminishing function of magnetic field M , non-uniform heat source A, B and thermal radiation R parameters. Further, rate of thermal transport is more declined in nanofluid case as compared with hybrid nanofluids. And for additional values of n and We thermal transfer rate is boosted more in hybrid nanofluids when compared with mono nanofluids. Table 4 illustrates the validation of the present results of Nusselt number with power law index parameter in comparison with the results of Jafar et al. [22].

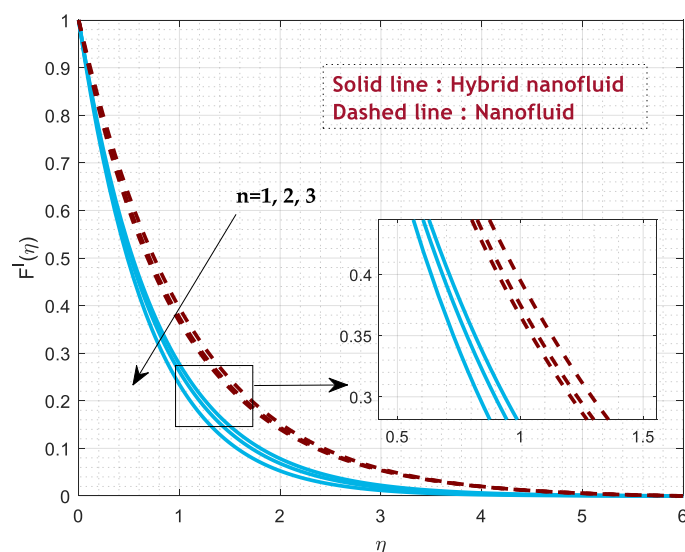


Fig. 2 Response of $F'(\eta)$ with n

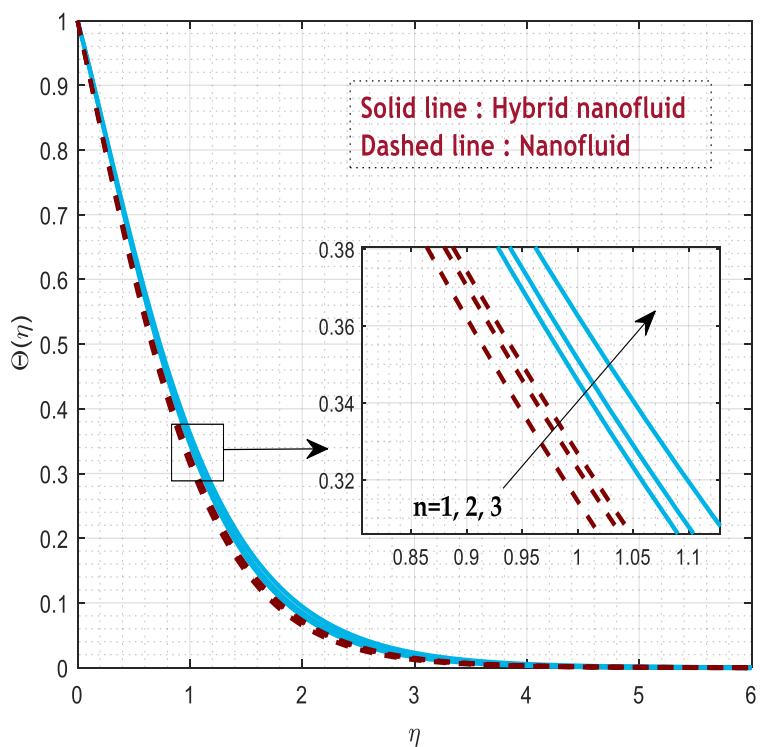


Fig. 3 Response of $\Theta(\eta)$ with n

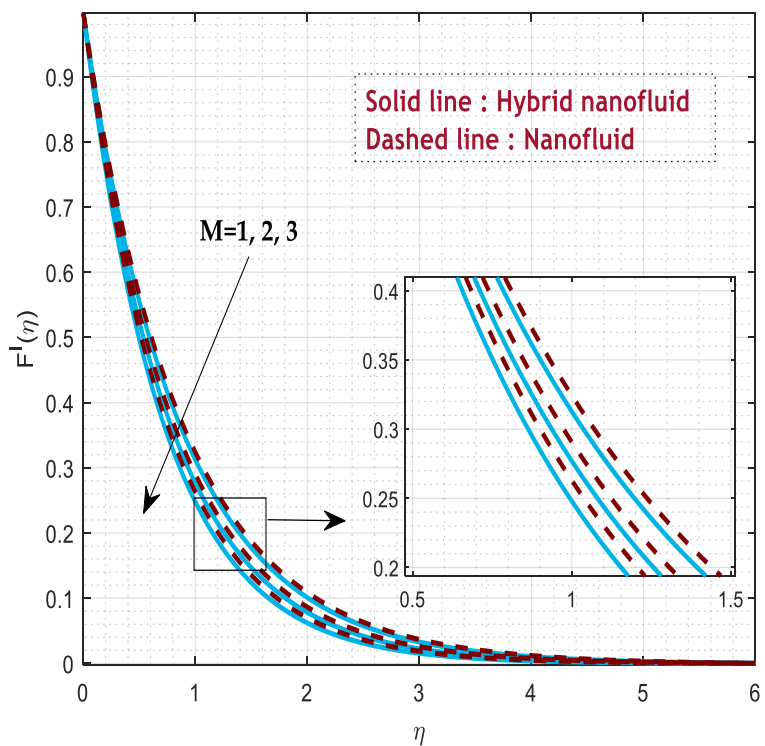


Fig. 4 Response of $F'(\eta)$ with M

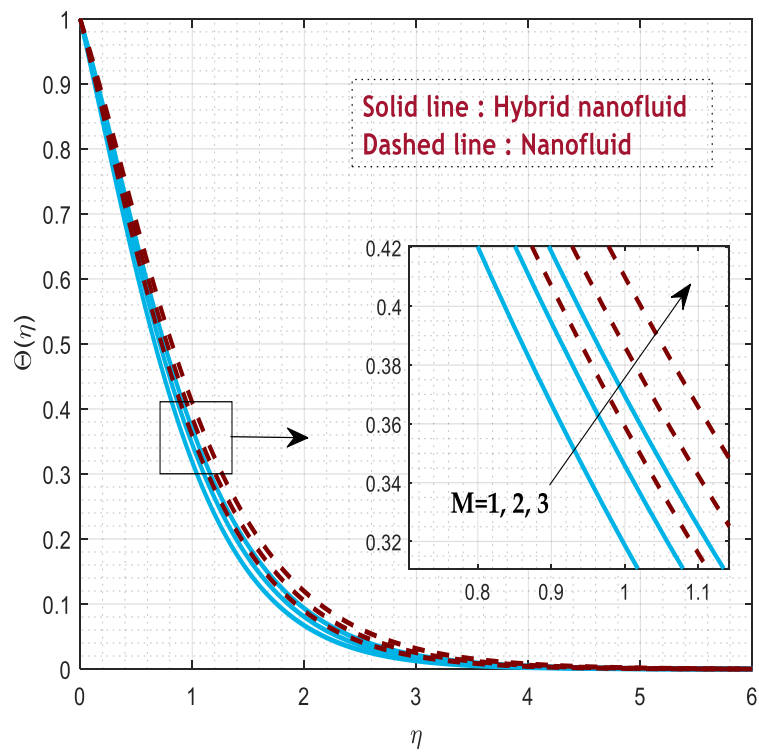


Fig. 5 Response of $\Theta(\eta)$ with M

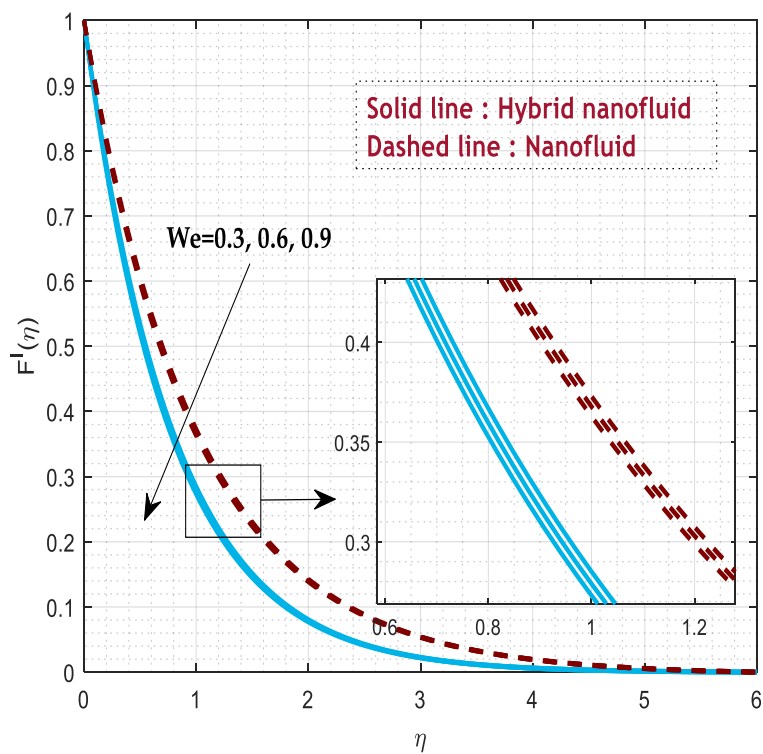


Fig. 6 Response of $F'(\eta)$ with We

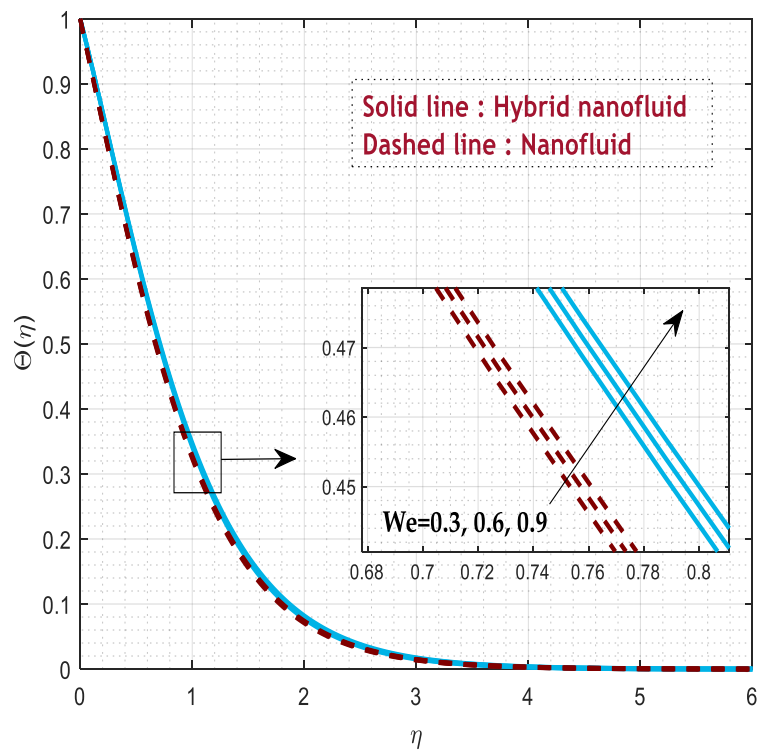


Fig. 7 Response of $\Theta(\eta)$ with We

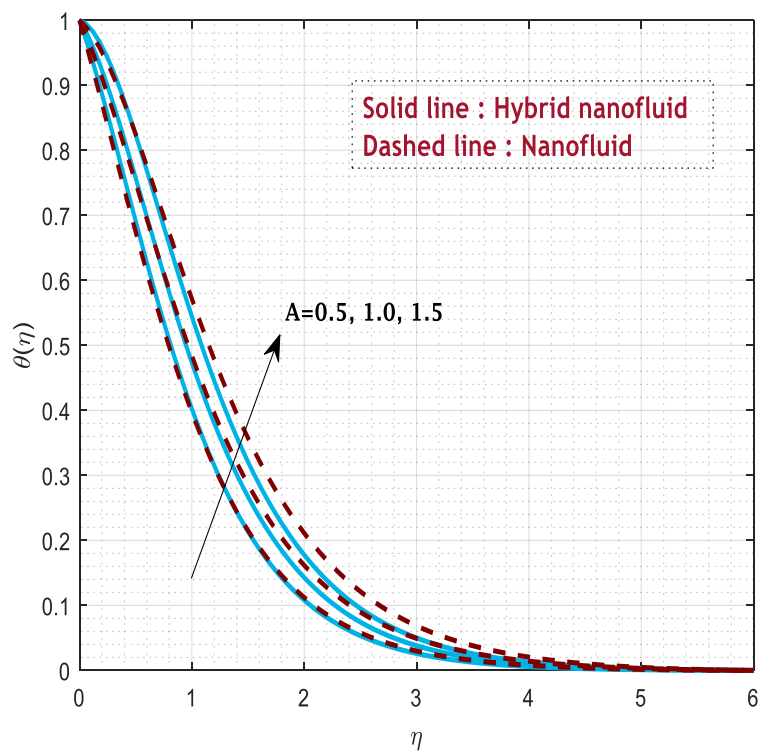


Fig. 8 Response of $\Theta(\eta)$ with A

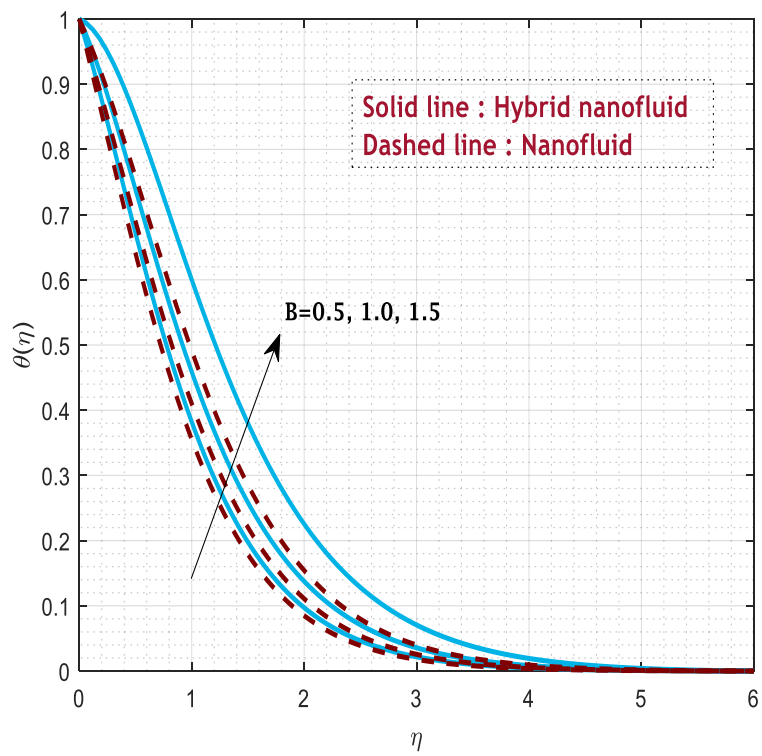


Fig. 9 Response of $\Theta(\eta)$ with B

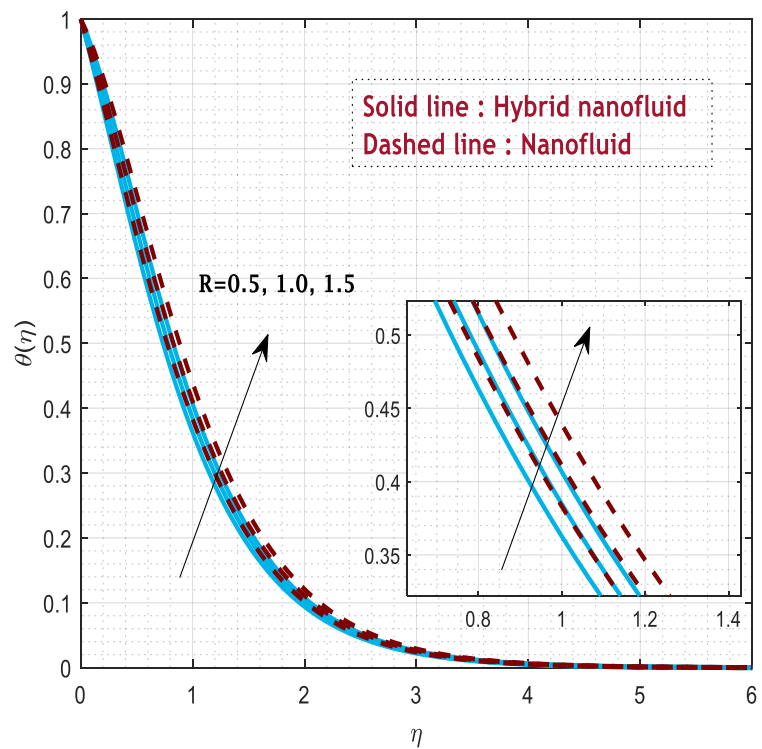


Fig. 10 Response of $\Theta(\eta)$ with R

Table 1 Physio-thermal characteristic of nanoparticles and the base liquid [23].

| Physical Property | MoS_2 | Ag | EG |
|-------------------|-----------------------|-------------------|----------------------|
| $C_p (J / KgK)$ | 397.21 | 235 | 2430 |
| $\sigma (S / m)$ | 2.09×10^{-5} | 6.3×10^7 | 4.3×10^{-5} |
| $\rho (Kg / m^3)$ | 5060 | 10480 | 1113.5 |
| $k (W / mK)$ | 904.4 | 429 | 0.253 |

Table 2 Variation in C_{fx} for nano and hybrid nanofluid cases.

| M | n | We | R | C_{fx} | |
|-----|-----|------|-----|------------------|-----------|
| | | | | Hybrid Nanofluid | Nanofluid |
| 1 | | | | -3.095112 | -3.462548 |
| 2 | | | | -3.383539 | -3.764055 |
| 3 | | | | -3.644778 | -4.038877 |
| | 1 | | | -1.829200 | -1.369722 |
| | 2 | | | -2.608818 | -2.252020 |
| | 3 | | | -3.383539 | -3.125965 |
| | | 0.3 | | -3.462144 | -3.182167 |
| | | 0.6 | | -3.344565 | -3.098033 |
| | | 0.9 | | -3.228998 | -3.014923 |
| | | | 0.5 | -1.829200 | -4.634648 |
| | | | 1.0 | -1.829200 | -4.634648 |
| | | | 1.5 | -1.829200 | -4.634648 |

Table 2 Variation in Nu_x for nano and hybrid nanofluid cases.

| M | n | We | A | B | R | Nu_x | |
|-----|-----|------|-----|-----|-----|------------------|-----------|
| | | | | | | Hybrid Nanofluid | Nanofluid |
| 1 | | | | | | 2.123669 | 2.031259 |
| 2 | | | | | | 1.858171 | 1.778990 |
| 3 | | | | | | 1.619385 | 1.552958 |
| | 1 | | | | | 1.242326 | 0.863747 |
| | 2 | | | | | 1.833623 | 1.321566 |
| | 3 | | | | | 2.426268 | 1.778990 |

| | | | | | | | |
|--|--|-----|-----|-----|-----|----------|----------|
| | | 0.3 | | | | 2.418843 | 1.772832 |
| | | 0.6 | | | | 2.429998 | 1.782061 |
| | | 0.9 | | | | 2.441256 | 1.791238 |
| | | | 0.5 | | | 1.862920 | 1.310351 |
| | | | 1.0 | | | 1.158736 | 0.724555 |
| | | | 1.5 | | | 0.454560 | 0.138754 |
| | | | | 0.4 | | 2.163591 | 1.495074 |
| | | | | 0.8 | | 1.704655 | 0.969143 |
| | | | | 1.2 | | 1.113427 | 0.168277 |
| | | | | | 0.5 | 2.335577 | 0.863747 |
| | | | | | 1.0 | 1.795538 | 0.677945 |
| | | | | | 1.5 | 1.255500 | 0.492143 |

Table 4 validation of results for Nusselt number with power law index parameter.

| n | Nu_x | |
|------|------------------|-----------------|
| | Jafar et al.[22] | Present Results |
| 0.75 | 3.1231 | 3.123258 |
| 1.5 | 3.5660 | 3.566120 |
| 7.0 | 4.1846 | 4.184254 |
| 10 | 4.2539 | 1.425398 |

4. Conclusion

The obtained outcomes are as follows:

- The hybrid nanofluid is more effective than the single nanofluid in heat transport properties.
- The size of the volume fraction impacts the development of the thermal profile.
- The enhancement in magnetic properties develops the resistance power to reduce the velocity profile and to enhance the heat flow rate.
- Increasing the stretching parameter depreciates the velocity profile and enhances the heat rate.
- The radiation effect increases the heat transfer rate.

5. References

- [1] S.U.S. Choi, J.A. Eastman, Enhancing thermal conductivity of fluids with nanoparticles, ASME International Mechanical Engineering Congress and Exposition. San Francisco, CA. 66 (1995) 99–105. doi:10.1115/1.1532008.
- [2] I. Fersadou, H. Kahalerras, M. El Ganaoui, MHD mixed convection and entropy generation of a nanofluid in a vertical porous channel, *Comput. Fluids*. 121 (2015) 164–179. <https://doi.org/10.1016/j.compfluid.2015.08.014>.
- [3] P.M. Patil, M. Kulkarni, P.S. Hiremath, Effects of surface roughness on mixed convective nanofluid flow past an exponentially

- stretching permeable surface, Chinese J. Phys. 64 (2020) 203–218. <https://doi.org/10.1016/j.cjph.2019.12.006>.
- [4] P. Sudarsana Reddy, A.J. Chamkha, A. Al-Mudhaf, MHD heat and mass transfer flow of a nanofluid over an inclined vertical porous plate with radiation and heat generation/absorption, Adv. Powder Technol. 28 (2017) 1008–1017. <https://doi.org/10.1016/j.apt.2017.01.005>.
- [5] S.P. Samrat, C. Sulochana, G.P. Ashwinkumar, Impact of Thermal Radiation on an Unsteady Casson Nanofluid Flow over a Stretching Surface, Int. J. Appl. Comput. Math. 5 (2019). <https://doi.org/10.1007/s40819-019-0606-2>.
- [6] H. Waqas, S.M. Raza Shah Naqvi, M.S. Alqarni, T. Muhammad, Thermal transport in magnetized flow of hybrid nanofluids over a vertical stretching cylinder, Case Stud. Therm. Eng. 27 (2021) 101219. <https://doi.org/10.1016/j.csite.2021.101219>.
- [7] U. Rashid, H. Liang, H. Ahmad, M. Abbas, A. Iqbal, Y.S. Hamed, Study of (Ag and TiO₂)/water nanoparticles shape effect on heat transfer and hybrid nanofluid flow toward stretching shrinking horizontal cylinder, Results Phys. 21 (2021) 103812. <https://doi.org/10.1016/j.rinp.2020.103812>.
- [8] H. Ullah, T. Hayat, S. Ahmad, M. Sh. Alhodaly, S. Momani, Numerical simulation of MHD hybrid nanofluid flow by a stretchable surface, Chinese J. Phys. 71 (2021) 597–609. <https://doi.org/10.1016/j.cjph.2021.03.017>.
- [9] A. Jamaludin, K. Naganthran, R. Nazar, I. Pop, MHD mixed convection stagnation-point flow of Cu-Al₂O₃/water hybrid nanofluid over a permeable stretching/shrinking surface with heat source/sink, Eur. J. Mech. B/Fluids. 84 (2020) 71–80. <https://doi.org/10.1016/j.euromechflu.2020.05.017>.
- [10] C. Sulochana, S.P. Samrat, N. Sandeep, International Journal of Mechanical Sciences Boundary layer analysis of an incessant moving needle in MHD radiative nano fluid with joule heating, 129 (2017) 326–331.
- [11] I. Tlili, S.P. Samrat, N. Sandeep, A computational frame work on magnetohydrodynamic dissipative flow over a stretched region with cross diffusion: Simultaneous solutions, Alexandria Eng. J. 60 (2021) 3143–3152. <https://doi.org/10.1016/j.aej.2021.01.052>.
- [12] I. Waini, A. Ishak, I. Pop, Flow and heat transfer of a hybrid nanofluid past a permeable moving surface, Chinese J. Phys. 66 (2020) 606–619. <https://doi.org/10.1016/j.cjph.2020.04.024>.
- [13] F. Mabood, MHD boundarylayer flowandheattransferofnanofluids overanonlinearstretchingsheet: Anumericalstudy, (2014).
- [14] T. Hayat, M.Z. Kiyani, A. Alsaedi, M. Ijaz Khan, I. Ahmad, Mixed convective three-dimensional flow of Williamson nanofluid subject to chemical reaction, Int. J. Heat Mass Transf. 127 (2018) 422–429. <https://doi.org/10.1016/j.ijheatmasstransfer.2018.06.124>.
- [15] I. Tlili, H.A. Nabwey, S.P. Samrat, N. Sandeep, 3D MHD nonlinear radiative flow of CuO-MgO/methanol hybrid nanofluid beyond an irregular dimension surface with slip effect, Sci. Rep. 10 (2020) 1–14. <https://doi.org/10.1038/s41598-020-66102-w>.

- [16] W. Alghamdi, A. Alsubie, P. Kumam, A. Saeed, T. Gul, MHD hybrid nanofluid flow comprising the medication through a blood artery, *Sci. Rep.* 11 (2021) 1–13. <https://doi.org/10.1038/s41598-021-91183-6>.
- [17] M. Shoaib, M.A.Z. Raja, M.T. Sabir, S. Islam, Z. Shah, P. Kumam, H. Alrabaiah, Numerical investigation for rotating flow of MHD hybrid nanofluid with thermal radiation over a stretching sheet, *Sci. Rep.* 10 (2020) 1–15. <https://doi.org/10.1038/s41598-020-75254-8>.
- [18] E.H. Aly, I. Pop, MHD flow and heat transfer near stagnation point over a stretching/shrinking surface with partial slip and viscous dissipation: Hybrid nanofluid versus nanofluid, *Powder Technol.* 367 (2020) 192–205. <https://doi.org/10.1016/j.powtec.2020.03.030>.
- [19] G.P. Ashwinkumar, S.P. Samrat, N. Sandeep, Convective heat transfer in MHD hybrid nanofluid flow over two different geometries, *Int. Commun. Heat Mass Transf.* 127 (2021) 105563. <https://doi.org/10.1016/j.icheatmasstransfer.2021.105563>.
- [20] S.S. Ghadikolaei, M. Yassari, H. Sadeghi, K. Hosseinzadeh, D.D. Ganji, Investigation on thermophysical properties of Tio₂–Cu/H₂O hybrid nanofluid transport dependent on shape factor in MHD stagnation point flow, *Powder Technol.* 322 (2017) 428–438. <https://doi.org/10.1016/j.powtec.2017.09.006>.
- [21] N.Sandeep, S.P. Samrat, G.P. Ashwinkumar, Flow and heat transfer in radiative MHD dusty-hybrid ferrofluids, *Waves in Random and Complex Media.* (2022) 1–14.
- [22] A.B. Jafar, S. Shafie, I. Ullah, MHD radiative nanofluid flow induced by a nonlinear stretching sheet in a porous medium, *Heliyon.* 6 (2020) e04201. <https://doi.org/10.1016/j.heliyon.2020.e04201>.
- [23] E.A. Algehyne, E.R. El-Zahar, S.H. Elhag, F.S. Bayones, U. Nazir, M. Sohail, P. Kumam, Investigation of thermal performance of Maxwell hybrid nanofluid boundary value problem in vertical porous surface via finite element approach, *Sci. Rep.* 12 (2022) 1–12. <https://doi.org/10.1038/s41598-022-06213-8>.